Density Functional Theory Calculations on the Dielectric Constant Dependence of the Oxidation Potential of Chlorophyll: Implication for the High Potential of P680 in Photosystem II†

Koji Hasegawa*,‡ and Takumi Noguchi*,§

Laboratory for Photo-Biology (I), RIKEN Photodynamics Research Center, Aoba, Sendai, Miyagi 980-0845, Japan, and Institute of Materials Science, University of Tsukuba, Tsukuba, Ibaraki 305-8573, Japan

Received February 15, 2005; Revised Manuscript Received April 4, 2005

ABSTRACT: The primary donor chlorophyll (Chl) of photosystem II (PSII), P680, has an extremely high oxidation redox potential (E_{ox}) of ∼1.2 V, which is essential for photosynthetic water oxidation. The mechanism for achieving a high potential such as that of P680 has been one of the central questions in photosynthesis research. Here, we have examined the dielectric constant (ϵ) dependence of the E_{ox} of monomer Chl using density functional theory calculations with the polarizable continuum model. The calculated E_{ox} of a model Chl compound exhibited a sharp increase with a decrease in ϵ in the relatively low ϵ region ($\epsilon < 5$). In contrast, in the higher-ϵ region, E_{ox} was rather insensitive to ϵ and converged to a constant value at very high ϵ values. This tendency in the high-ϵ region explains the experimental E_{ox} values of isolated Chl *a* that have been observed in a relatively narrow range of 0.74−0.93 V. The E_{ox} of Chl in an ideal hydrophobic protein was estimated to be ∼1.4 V at an ϵ value of 2. This value indicates that Chl in a hydrophobic environment originally has a high E_{ox} that is sufficient for oxidizing water ($E_{ox} = 0.88$ V at pH 6). On the basis of the reported X-ray crystallographic structures, the protein environment of P680 in PSII was estimated to be more hydrophobic than that of the primary donors in bacterial reaction centers. It is therefore suggested that the low-dielectric environment around P680 is one of the major factors in its very high E_{ox}, and thus, introducing nonpolar amino acids into the binding pocket of P680 was an important process in the evolution of PSII.

Photosynthetic water oxidation began at least 2.5−2.6 billion years ago by cyanobacteria (*1*, *2*). Utilization of water as a terminal electron donor for reduction of carbon dioxide to synthesize sugar was an ultimate strategy for early photosynthetic life to survive on Earth. The beginning of water oxidation was also a turning point in the evolution of other life on Earth; molecular oxygen released as a byproduct made the atmosphere aerobic, leading to the extensive development of life.

Water oxidation is carried out in photosystem II (PSII),[1] which is thought to be developed from the type II reaction center (RC) of anoxygenic photosynthetic organisms or homodimeric RC as a common ancestor (*2*−*5*). During the evolution of PSII, two major events were necessary to gain the water-oxdizing capability: creation of the catalytic site, the so-called Mn cluster, and increasing the oxidation redox potential (E_{ox}) of the primary donor chlorophyll (Chl) to a level sufficient for water oxidation (*3*, *5*). The primary donor of purple photosynthetic bacteria, e.g., P870 of *Rhodobacter sphaeroides*, has an E_{ox} of ∼0.5 V (*6*), which is far below the potential of water oxidation of 0.88 V at pH 6, the pH showing the maximum O_2-evolving activity in PSII preparations (*7*) (Figure 1). In contrast, the primary donor of PSII, P680, is estimated to have an extremely high E_{ox} of 1.1−1.3 V (Figure 1) (*8*−*11*). This value is much higher than the potentials of any other primary donors, and even higher than the E_{ox} values of isolated Chl *a* in organic solvents [0.74−0.93 V (*12*−*20*)] (Figure 1). How this extremely high potential of P680 was achieved during the evolution of PSII has been one of the central questions in photosynthetic research (*3*, *5*, *21*−*25*).

Several mechanisms have been proposed for increasing E_{ox} in the development of P680. One effective way is changing the constituting pigment (*3*). Indeed, the E_{ox} of Chl *a* is higher than that of Bchl *a* by 0.1−0.2 V (*17*, *20*), although this difference is not enough to explain the potential gap of ∼0.7 V between P870 and P680 (Figure 1). Also, weak electronic coupling in the Chl *a* dimer has been suggested as a major reason for the high E_{ox} of P680 (*5*, *24*, *25*). Charge delocalization over the dimer in a primary donor cation decreases its E_{ox} (*26*−*29*), and hence, the rather

† This work was supported by grants for the Frontier Research System and Special Postdoctoral Researchers Programs at RIKEN, a Grant-in-Aid for Young Scientists (B) (15770101) from MEXT of Japan to K.H., Special Research Project "NanoScience" at the University of Tsukuba, and a Grant-in-Aid for Scientific Research (14540607) from MEXT of Japan to T.N.

* To whom correspondence should be addressed. K.H.: phone, +81-22-228-2047; fax, +81-22-228-2045; e-mail, kojihase@postman.riken.go.jp. T.N.: phone, +81-29-853-5126; fax, +81-29-855-7440; e-mail, tnoguchi@ims.tsukuba.ac.jp.

‡ RIKEN Photodynamics Research Center.

§ University of Tsukuba.

[1] Abbreviations: Bchl, bacteriochlorophyll; Chl, chlorophyll; DFT, density functional theory; IP, ionization potential; P680, primary donor of photosystem II; PCM, polarizable continuum model; PSII, photosystem II; RC, reaction center; SHE, standard hydrogen electrode.

10.1021/bi050273c CCC: $30.25
Published on Web 05/19/2005

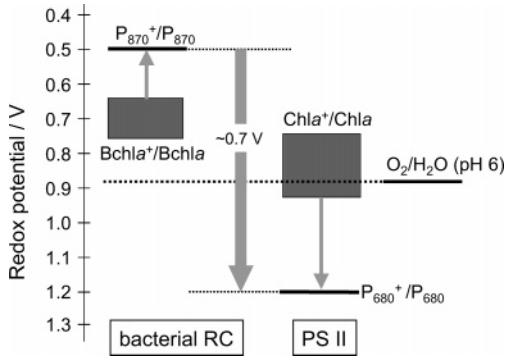

FIGURE 1: Comparison of the redox potential of $P680^+/P680$ in PSII with the potentials of $P870^+/P870$ in the RC of *Rb. sphaeroides*, Chl a^+/Chl *a* and Bchl a^+/Bchl *a* in organic solvents, and water (O_2/H_2O at pH 6.0). The redox potentials of Chl a^+/Chl *a* and Bchl a^+/Bchl *a* in solvents are distributed in some potential range depending on solvent species.

monomeric nature of P680 (*30*−*32*) should provide a potential higher than that of the strongly coupled dimer like P870. However, this mechanism of weak coupling cannot fully explain the E_{ox} of P680 that is even higher than the reported E_{ox} of monomeric Chl *a* by 0.3−0.5 V (Figure 1).

Another simple mechanism for increasing the E_{ox} is placing positively charged amino acid groups near P680. D2-Arg181 has been proposed to be the candidate for such an amino acid residue (*23*). According to the recently published X-ray structure of PSII (*33*), however, no charged amino acids are found in the vicinity of P680 and the D2-Arg181 side group is more than 13 Å from the Mg atom of P680, the distance at which strong screening effects for attenuating the electrostatic interactions have been observed in bacterial RCs (*34*, *35*).

There is one missing consideration in the above argument. Does monomeric Chl *a* in typical photosynthetic proteins indeed have an E_{ox} value in the potential range of Chl *a*, 0.74−0.93 V, that has been determined in organic solvents? In electrochemical measurements, polar solvents with high dielectric constants must be used to dissolve supporting electrolytes. In contrast, it is known that the local dielectric constant in the protein interior is generally low (*36*−*41*). In particular, Chl molecules bound to photosynthetic proteins usually exist in hydrophobic environments with quite low dielectric constants (*37*). In this respect, Rutherford and Faller (*5*) recently proposed that the E_{ox} of monomer Chl is intrinsically high in the dielectric environment of a RC protein. Also, very recently, Ishikita et al. (*42*) calculated the redox potentials of P680 and other Chl molecules in PSII RCs considering the protein environment, and showed the importance of the low-dielectric environment around P680 in realizing the high potential of P680. However, a clear view of the relationship between the E_{ox} of Chl and the surrounding dielectric property has not yet been obtained. Clarifying this relationship therefore should provide an important basis for understanding the mechanism of the extremely high E_{ox} of P680.

In this study, the dielectric constant (ϵ) dependence of the E_{ox} of Chl was calculated using the density functional theory (DFT) method with the polarizable continuum model (PCM). DFT calculations have recently been applied to Chl-related molecules, and successfully provided information about the electronic, magnetic, and vibrational properties of their cation and anion radicals as well as those of neutral species (*43*−*53*). Although solvation effects have been treated in some quantum chemical calculations (*44*, *53*−*56*), systematic investigation on this subject has not yet been performed. From the calculated ϵ dependence, the E_{ox} of Chl in a nonpolar environment ($\epsilon = 2$) representing the interior of hydrophobic proteins was estimated. On the basis of the results that were obtained, the reason for the high potential of P680 and the strategy for increasing the potential in the evolution of PSII are discussed.

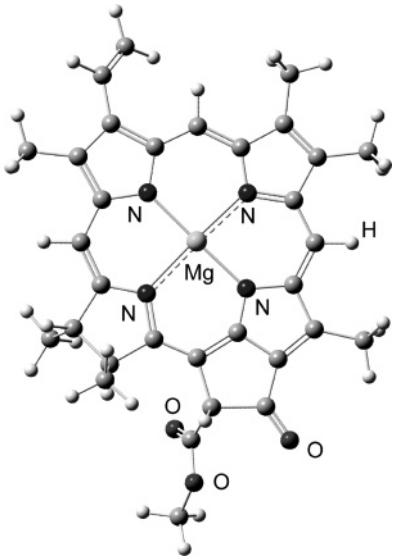

FIGURE 2: Structure of model Chl used in this study.

COMPUTATIONAL METHODS

All calculations were performed in GAUSSIAN 03 (*57*). The initial coordinates of atoms in the model Chl compound (Figure 2) were obtained from the crystal structure of ethyl chlorophyllide *a* (*58*). Geometry optimization was carried out for both neutral Chl and its cation radical (Chl^+) by the restricted and unrestricted DFT method, respectively, using Becke's three-parameter hybrid functional (*59*) combined with the Lee−Yang−Parr correlation functional (*60*) (B3LYP) and the 6-31G(d) basis set. Final electronic energies were calculated at the B3LYP/6-311+G(d) level for the optimized structures. These calculations were performed in the gas phase and in solvents approximated with IEF−PCM (PCM calculation using the integrated equation formalism model) (*61*−*63*). Seven solvent parameters included in GAUSSIAN 03 were used: argon ($\epsilon = 1.4$), benzene ($\epsilon = 2.2$), chloroform ($\epsilon = 4.9$), dichloroethane ($\epsilon = 10.4$), acetone ($\epsilon = 20.7$), dimethyl sulfoxide ($\epsilon = 46.7$), and water ($\epsilon = 78.4$).

RESULTS

The structure of the model Chl, whose geometry was optimized at the B3LYP/6-31G(d) level, is shown in Figure 2. This Chl model retains the structure of Chl *a* except for the phytyl ester side chain and ethyl group, which are replaced with a methyl group to reduce the number of atoms. Table 1 summarizes the results of energy calculations of Chl and Chl^+ in the gas phase and in various solvents with different ϵ values. The ϵ dependence of the electronic energies (E_{elec}) of Chl and Chl^+ is depicted in Figure 3.

Table 1: Calculated Electronic Energies, Ionization Potentials, and Oxidation Redox Potentials of Model Chl in Solvents with Different Dielectric Constants

	E_{elec} (eV)[b]				
ϵ[a]	Chl	Chl^+	IP (eV)[c]	E_{ox}^{cal} (V)[d]	E_{ox}^{cor} (V)[e]
1.0	−51234.240	−51228.010	6.230	1.80	1.96
1.4	−51234.407	−51228.530	5.877	1.45	1.61
2.2	−51234.583	−51229.007	5.576	1.15	1.31
4.9	−51234.854	−51229.568	5.286	0.86	1.02
10.4	−51234.014	−51229.874	5.141	0.71	0.87
20.7	−51235.108	−51230.043	5.065	0.64	0.80
46.7	−51235.155	−51230.114	5.041	0.61	0.77
78.4	−51235.262	−51230.260	5.002	0.57	0.73

[a] Dielectric constants of the gas phase (1.0), argon (1.4), benzene (2.2), chloroform (4.9), dichloroethane (10.4), acetone (20.7), dimethyl sulfoxide (46.7), and water (78.4). [b] Electronic energies of Chl and Chl^+ calculated at the B3LYP/6-311+G(d) level for their optimized geometries obtained at the B3LYP/6-31G(d) level in solvents. [c] Ionization potential obtained as the difference between the E_{elec} values of Chl and Chl^+. [d] Calculated redox potential vs the SHE of the Chl^+/Chl redox couple. The absolute potential of the SHE was assumed to be 4.43 V (*68*, *69*). [e] Corrected redox potential obtained by adding a constant (0.16 V) to E_{ox}^{cal} to fit to the experimental potentials of Chl *a* in organic solvents (see Figure 4).

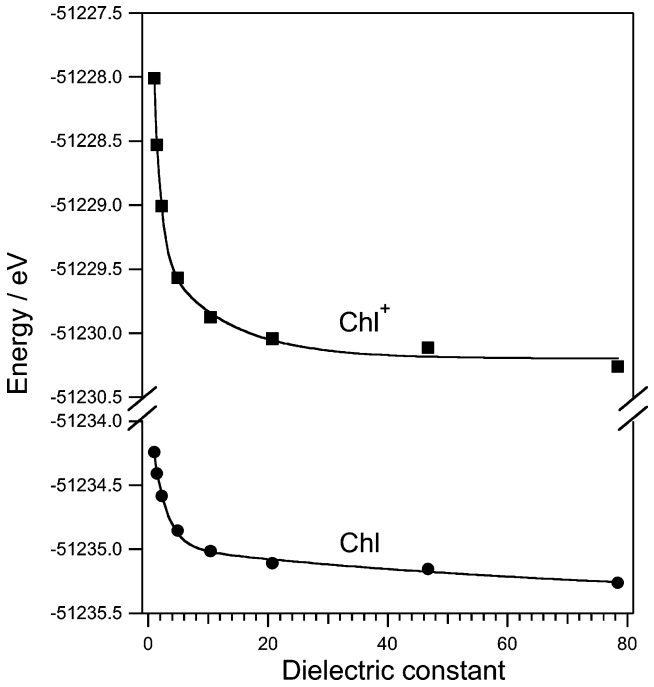

FIGURE 3: Calculated electronic energies (E_{elec}) of Chl (●) and Chl^+ (■) as a function of the dielectric constant.

Although the E_{elec} values of Chl and Chl^+ were rather insensitive to ϵ in the higher-ϵ region, they rapidly increased as ϵ was lowered in the relatively low-ϵ region ($\epsilon < 5$). This ϵ dependency of E_{elec} was more prominent in Chl^+ than in Chl.

The ionization potential (IP) of Chl at each dielectric constant was estimated as the difference in E_{elec} values between Chl and Chl^+ (fourth column of Table 1). The IP value in the gas phase was estimated to be 6.230 eV. This value is in good agreement with the IP of 6.1 eV for Chl *a* in the gas phase previously estimated from the measurement of the photocurrent threshold in solution (*64*) and the IPs of ~6 eV for various chlorin compounds in previous ab initio MO calculations (*43*, *44*, *48*, *65*, *66*).

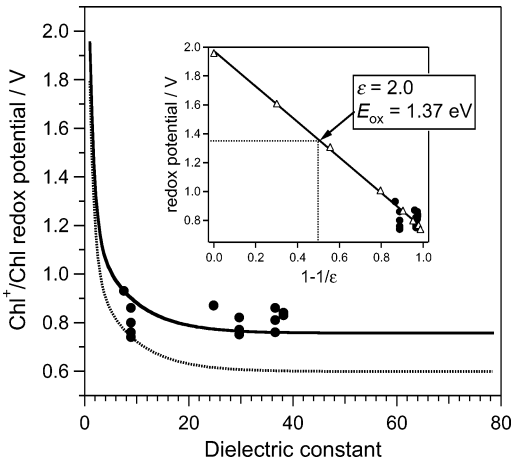

FIGURE 4: Calculated oxidation redox potential (E_{ox}^{cal}) of model Chl (•••) as a function of the dielectric constant (ϵ) in comparison with the experimental potentials of Chl *a* in organic solvents (●). The solid line expresses the corrected redox potential (E_{ox}^{cor}) of Chl obtained by adding a constant to E_{ox}^{cal} to fit to the experimental potentials. The inset shows E_{ox}^{cor} values of Chl in various solvents (△; Table 1) plotted as a function of $1 - 1/\epsilon$, showing a linear relationship. The experimental data are also plotted in this graph (●). The estimated E_{ox}^{cor} value at an ϵ of 2 is given.

The standard redox potential versus the standard hydrogen electrode (SHE), $E°$(SHE), can be converted from the electronic energy on an absolute scale, E(abs), by the following equation (*54*, *67*, *68*)

$$E°(\text{SHE}) = E(\text{abs}) - E_H$$

where E_H is the absolute potential of SHE referenced to vacuum, which has been estimated to be 4.43 V (*68*, *69*). Because E(abs) corresponds to the IP of the reduced species (*67*), the standard redox potential versus the SHE of the Chl^+/Chl couple, E_{ox}, can be estimated from the IP of Chl by the equation

$$E_{ox} = \text{IP} - 4.43$$

The calculated E_{ox} (E_{ox}^{cal}) at each ϵ is presented in Table 1 (fifth column), and the E_{ox}^{cal} curve as a function of ϵ is depicted in Figure 4 (•••). The E_{ox}^{cal} was estimated to be 1.80 V in the gas phase ($\epsilon = 1.0$), and it decreased dramatically with an increase in ϵ but finally converged to a constant value of ~0.6 V. Thus, E_{ox}^{cal} was highly sensitive to ϵ in the relatively low-ϵ region ($\epsilon < 5$), and became insensitive in the higher-ϵ region [Figure 4 (•••)].

Experimental values of the oxidation potential of Chl *a* measured in various aprotic solvents (*12*−*20*) are also plotted in Figure 4 (●). These measurements were performed in tetrahydrofuran ($\epsilon = 7.5$), dichloromethane ($\epsilon = 8.9$), butyronitrile ($\epsilon = 24.8$), propionitrile ($\epsilon = 29.7$), acetonitrile ($\epsilon = 36.6$), and dimethylformamide ($\epsilon = 38.2$) as solvents. These experimental potentials range between 0.93 and 0.74 V. The calculated E_{ox}^{cal} of the model Chl in the ϵ range of 7−40 was 0.78−0.60 V [Table 1 and Figure 4 (•••)]. This result is in satisfactory agreement with the experimental data, although calculations provided values lower by ~0.15 V than those from the experiments. This deviation is at the same level of the average errors (~0.18 eV) of the absolute IP values by the B3LYP method previously estimated for various small molecules (*70*, *71*). Selection of a basis set

[6-311+G(d)] also influences the calculated values. In fact, the smaller basis set of 6-31G(d) provided further smaller E_{ox}^{cal} values (by ~0.28 V) in the gas phase. The necessity of using a large basis set to obtain a reliable potential of Chl has been pointed out in the previous DFT study (*44*). It should be emphasized, however, that what is important in our study is not the absolute value of the calculated E_{ox}^{cal} but its change depending on ϵ. The observed ϵ dependence of E_{ox}^{cal} was a general tendency even in calculations with a smaller basis set and for different Chl models, including those with a more truncated chlorin ring, with a water ligand to Mg, and with a bacteriochlorin ring (not shown).

To correct the errors in the absolute E_{ox}^{cal} values, an appropriate constant was added to the E_{ox}^{cal} curve [Figure 4 (•••)] to fit to the experimental potentials. The best fit was achieved with the constant of 0.16 V, and the corrected E_{ox} (E_{ox}^{cor}) curve as a function of ϵ is shown in Figure 4 with a solid line. The relatively large deviation of the experimental data at an ϵ of 8.9 (dichloromethane) from the E_{ox}^{cor} curve could originate from partial aggregation of Chl *a* in dichloromethane that does not provide a fifth ligand to Mg. The E_{ox}^{cor} was 1.96 V in the gas phase ($\epsilon = 1.0$) and converged to ~0.74 V at very high ϵ values. Crystal and Friesner (*44*) previously calculated the solvation energy for model Bchl in dimethylformamide ($\epsilon = 38.2$) at the B3LYP/6-31G(d,p) level and obtained a value of approximately −1.3 V, which is similar to our result of approximately −1.2 V at the same ϵ. The E_{ox}^{cor} values for various solvents (Table 1, sixth column) plotted against $1 - 1/\epsilon$ [Figure 4 inset (△)] showed a linear relationship, in agreement with Born's theory (*72*).

DISCUSSION

The dielectric constant of proteins comprises electronic polarization (high-frequency dielectric constant or optical dielectric constant) and reorientation of polar protein groups (*36*, *39*−*41*). Since such reorientations of chemical groups are rather restricted in the protein matrix, local dielectric constants of the protein interior are generally low (*36*−*41*). This is the case particularly for hydrophobic proteins such as photosynthetic RCs (*37*, *40*). If we assume that a Chl molecule exists in an ideal hydrophobic protein that does not include any polar amino acid groups, then the dielectric property of the Chl binding site would be attributed only to the electronic polarization of the surrounding groups. In this case, the local dielectric constant of the Chl site will be regarded as being ~2, which is a general value of the optical dielectric constant of organic molecules (*36*, *39*).

From the obtained dependency of E_{ox}^{cor} on ϵ (Figure 4), the E_{ox} of Chl at an ϵ of 2.0 can be estimated to be 1.37 V (Figure 4 inset). Thus, it is concluded that in the nonpolar environment of an ideal hydrophobic protein, Chl originally has a very high potential of ~1.4 V. This value, which is much higher than the generally accepted E_{ox} of monomer Chl (~0.8 V) in organic solvents (*12*−*20*), is sufficiently high for Chl to oxidize water ($E_{ox} = 0.88$ V at pH 6.0). This estimation also indicates that the E_{ox} of P680, which has been estimated to be ~1.2 V (*8*−*11*), is only slightly (by ~0.2 V) lower than the E_{ox} of monomer Chl in an ideal hydrophobic environment (Figure 5). In contrast, the E_{ox} of P700 [~0.5 V (*73*)] is significantly lower (by ~0.9 V) than this original potential of Chl. The E_{ox} of Bchl *a* in an ideal

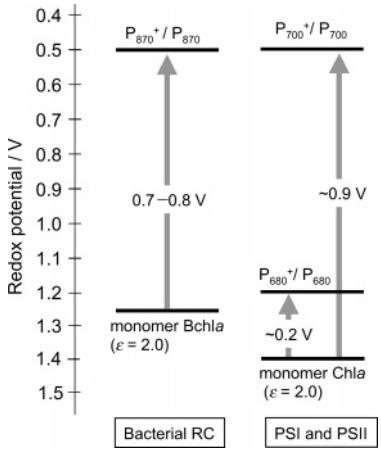

FIGURE 5: Relationship of the oxidation redox potentials of Chl *a* and Bchl *a* in a nonpolar environment ($\epsilon = 2$) with those of P680 in PSII, P700 in PSI, and P870 in the bacterial RC.

hydrophobic environment is assumed to be ~1.2−1.3 V, taking into account the potential gap of 0.1−0.2 V between Chl *a* and Bchl *a* in organic solvents (*17*, *20*). Thus, the E_{ox} of P870, ~0.5 V (*6*), is lower than this E_{ox} of Bchl *a* in a hydrophobic protein by 0.7−0.8 V (Figure 5). The question from this potential scheme is now the reasons for the smaller potential decrease in P680 in comparison with those of other primary donors.

Table 2 lists the polar amino acid groups [whose dipole moments are higher than 1.0 D (*74*)], and the carbonyl and ester groups of Chl molecules surrounding P680, P870, and P700, which were selected on the basis of the X-ray structures of PSII from *Thermosynechococcus elongatus* (PDB entry 1S5L) (*33*), the RC from *Rb. sphaeroides* (PDB entry 1AIJ) (*75*), and PSI from *T. elongatus* (PDB entry 1JBO) (*76*), respectively. The O, N, or S atoms of these side chains and polar groups are within 7 Å of the C, N, O, or Mg atoms of the chlorin rings (rings I−V plus keto C_9═O and acetyl C_2═O groups, but without other side groups and a phytol chain). This 7 Å distance was adopted in an effort to select the chemical groups directly facing the primary donors, on the basis of the observation that the distance between the Mg atom and the α-carbon of its His ligand is ~6.5 Å in all the (B)Chls of these primary donors.

Nine polar amino acid groups and two keto C_9═O groups of accessory Chls (Chl_{D1} and Chl_{D2}) are found around P680, while 16 polar amino acids, two keto C_9═O groups of accessory Bchls (B_L and B_M), and two acetyl C_2═O groups of the partner Bchls of the dimer itself (P_L and P_M) are present around P870. It is noted that a similar number of polar groups, i.e., 18 polar amino acids and four C═O groups of Bchls, are found around P960 of *Rhodopseudomonas viridis* (PDB entry 1PRC) (*77*) (not shown). Thus, only half of the number of polar groups exist around P680 compared with the primary donors of purple bacteria. In addition, 13 polar amino acids, two keto C_9═O groups, and two carbomethoxy C_{10}═O groups of accessory Chls (eC-A2 and eC-B2) are present around P700 in PSI. It seems evident therefore that the environment of the binding pocket of P680 in PSII is much more hydrophobic than that of P870 (P960) and P700.

The above qualitative considerations suggest that the hydrophobic environment around P680 is one of the major reasons for its high potential, that is, the small potential

Table 2: Polar Amino Acid Side Chains and (B)Chl Groups Surrounding the Primary Donors

P680[a]		P870[b]		P700[c]	
polar groups[d]	*d* (Å)[e]	polar groups[d]	*d* (Å)[e]	polar groups[d]	*d* (Å)[e]
amino acid side chain		amino acid side chain		amino acid side chain	
D1-183M	3.8	L-158S	6.4	A-603Y	4.8
D1-187Q	5.6	L-160T	6.4	A-655W	6.3
D1-198H	2.4	L-162Y	5.5	A-680H	2.3
D1-286T	5.3	L-166N	5.0	A-683W	4.6
D2-186Q	5.8	L-168H	2.9	A-742T	4.8
D2-191W	3.5	L-173H	2.2	A-743T	3.0
D2-192T	5.1	L-244S	3.8	B-629Y	5.9
D2-197H	2.2	L-247C	5.2	B-631W	6.2
D2-282S	3.8	L-248M	3.6	B-634S	4.7
Chl		M-186T	5.2	B-660H	2.4
Chl_{D1} C_9=O	5.9	M-187N	5.7	B-663W	4.5
Chl_{D2} C_9=O	5.8	M-190S	3.8	B-726T	5.0
		M-195N	5.8	B-727Y	6.0
		M-202H	2.3	Chl	
		M-205S	3.7	eC-A2 C_9=O	3.4
		M-210Y	3.4	eC-A2 C_{10}OOMe	4.0
		Bchl		eC-B2 C_9=O	3.1
		P_L C_2=O	3.6	eC-B2 C_{10}OOMe	3.9
		P_M C_2=O	3.4		
		B_L C_9=O	6.4		
		B_M C_9=O	6.4		

[a] Based on the X-ray structure of PSII of *T. elongatus* by Ferreira et al. (*33*) (PDB entry 1S5L). [b] Based on the X-ray structure of the RC of *Rb. sphaeroides* by Stowell et al. (*75*) (PDB entry 1AIJ). [c] Based on the X-ray structure of PSI of *T. elongatus* by Jordan et al. (*76*) (PDB entry 1JBO). [d] Amino acid side chains with dipole moments larger than 1.0 D (*74*) are selected as polar residues. [e] Shortest distances between the O, N, or S atom of the polar groups and the C, N, O, or Mg atom of the (bacterio)chlorin ring, including the conjugated keto C_9=O group (and the acetyl C_2=O group for P870). Amino acid and Chl groups in which this distance is less than 7 Å are listed.

decrease form the original potential of monomer Chl in an ideal hydrophobic environment. A larger number of surrounding polar groups will increase the local dielectric constant of the binding pocket and decrease the potential of P870 (P960) and P700. Such dielectric effects of polar groups could be larger than those expected from their apparent numbers listed in Table 2, because of a greater likelihood that water and ions penetrate into the polar protein matrix. In addition to the dielectric effect, electrostatic interactions of the polar groups should directly affect the E_{ox}. It is noted, however, these electrostatic effects either decrease or increase the potentials. Indeed, recent calculations by Ishikita et al. (*42*) showed that the charges of amino acid side chains have a negative effect in total on the P680 potential, while the charges of cofactors contribute to its positive shift.

Another important factor in controlling the potential is dimerization of (B)Chl. Stabilization of the cation radical due to delocalization of a positive charge over the dimer decreases the E_{ox} of a primary donor (*26*−*29*). The extent of the E_{ox} decrease by charge delocalization has been estimated to be 0.13−0.18 V in P870 of *Rb. sphaeroides* from the E_{ox} upshifts in the HL(M202) and HL(L173) mutants (*78*−*80*). The primary donor in these mutants is a Bchl−Bph heterodimer with a positive charge localized on the Bchl side, whereas the charge in wild-type $P870^+$ is significantly delocalized. Also, charge delocalization in $P700^+$ has been proposed by FTIR studies (*81*).[2] In contrast, P680 has a relatively large separation of Chl molecules [Mg−Mg distance of 8.2−8.3 Å (*33*, *85*) in comparison with a distance of ∼7.6 Å in P870 (*75*)], and the positive charge has been suggested to be rather localized on the Chl on the D1 side (*30*−*32*), although partial delocalization is evident from the presence of a weak mid-IR intervalence band in $P680^+$ (*86*, *87*). Thus, the dimerization effect on the E_{ox} decrease may be small in P680, being consistent with the relatively smaller potential decrease of P680 from the calculated E_{ox} of monomeric Chl at an ϵ of 2 (Figure 5).

In the development of PSII from the bacterial RC (*2*−*5*), the E_{ox} of the primary donor had to dramatically increase by as much as ∼0.7 V to gain the capability of water oxidation (Figure 1). From the considerations given above, the major strategies for achieving this evolution are presumed to be as follows. (i) Replacing polar amino acid residues around the primary donor with nonpolar ones produces a more hydrophobic environment. Indeed, the number of polar amino acids was reduced almost to half in PSII (Table 2). This strategy of changing dielectric properties should be very effective in controlling the potential, because E_{ox} is highly sensitive to ϵ in the relatively low-ϵ region ($\epsilon < 5$), which might be realized in the photosynthetic proteins, and because the potential can be controlled within the range of ∼0.65 V (difference between ∼1.4 V at an ϵ of 2 and ∼0.75 V at very high ϵ values; Figure 4) by changing ϵ. (ii) Changing the charge distribution by polar groups around P increases its potential (*42*). (iii) Weakening the electronic coupling of the dimer decreases the extent of charge delocalization (*5*, *24*, *25*). This mechanism will upshift the potential by ∼0.15 V if complete charge localization is realized (*78*−*80*). (iv) Changing the pigment structure from Bchl *a* to Chl *a* (*3*) increases the potential by 0.1−0.2 V (*17*, *20*). Other factors such as distortion of the chlorin ring (*88*) might also contribute to the upshift of the potential. In contrast, the well-known hydrogen bond strategy for increasing the potential (*6*, *26*−*29*) seemed not to be adopted in the PSII evolution (*5*, *25*) judging from the free keto C=O interactions of P680 (*33*), possibly because this strategy conflicts with the hydrophobicity strategy described above.

In conclusion, this DFT calculation showed that Chl originally has a very high redox potential in a nonpolar environment, which is sufficient to oxidize water. The hydrophobic protein environment around P680 in PSII may be one of the major factors in achieving its high potential of ∼1.2 V. Further theoretical calculations explicitly including nearby amino acid residues and pigments will be needed to clarify the reason for the large potential difference between P680 and other primary donors.

ACKNOWLEDGMENT

We thank Professor Gernot Renger for valuable discussion and Dr. Taka-aki Ono for his kind support.

REFERENCES

1. Des Marais, D. J. (2000) Evolution: When did photosynthesis emerge on earth? *Science 289*, 1703−1705.

[2] Although EPR studies have shown that the spin density is largely localized on P_B (*82*), recent theoretical studies suggested that the spin asymmetry is generally larger than the charge asymmetry because of the spin polarization of the low-lying spin-paired π-orbitals (*83*, *84*).

2. Olson, J. M., and Blankenship, R. E. (2004) Thinking about the evolution of photosynthesis, *Photosynth. Res. 80*, 373−386.
3. Blankenship, R. E., and Hartman, H. (1998) The origin and evolution of oxygenic photosynthesis, *Trends Biochem. Sci. 23*, 94−97.
4. Xiong, J., and Bauer, C. E. (2002) Complex evolution of photosynthesis, *Annu. Rev. Plant Biol. 53*, 503−521.
5. Rutherford, A. W., and Faller, P. (2003) Photosystem II: Evolutionary perspectives, *Philos. Trans. R. Soc. London, Ser. B 358*, 245−253.
6. Lin, X., Murchison, H. A., Nagarajan, V., Parson, W. W., Allen, J. P., and Williams, J. C. (1994) Specific alteration of the oxidation potential of the electron donor in reaction centers from *Rhodobacter sphaeroides*, *Proc. Natl. Acad. Sci. U.S.A. 91*, 10265−10269.
7. Vass, I., and Styring, S. (1991) pH-Dependent charge equilibria between tyrosine-D and the S states in photosystem II. Estimation of relative midpoint redox potentials, *Biochemistry 30*, 830−839.
8. Jursinic, P., and Govindjee (1977) Temperature dependence of delayed light emission in the 6 to 340 microsecond range after a single flash in chloroplasts, *Photochem. Photobiol. 26*, 617−628.
9. Klimov, V. V., Allakhverdiev, S. I., Demeter, S., and Krasnovskii, A. A. (1979) Photoreduction of pheophytin in the photosystem 2 of chloroplasts with respect to the redox potential of the medium, *Dokl. Akad. Nauk SSSR 249*, 227−230.
10. Van Gorkom, H. J. (1985) Electron transfer in photosystem II, *Photosynth. Res. 6*, 97−112.
11. Rappaport, F., Guergova-Kuras, M., Nixon, P. J., Diner, B. A., and Lavergne, J. (2002) Kinetics and pathways of charge recombination in photosystem II, *Biochemistry 41*, 8518−8527.
12. Stanienda, A. (1965) Electrochemical investigations of chlorophylls a and b and of the pheophytins a and b, *Z. Phys. Chem. 229*, 257−272.
13. Kutyurin, V. M., Solov'ev, V. P., and Grigorovich, V. I. (1966) A study of reversible oxidation of chlorophyll and its derivatives by the polarographic method, *Dokl. Akad. Nauk SSSR 169*, 479−482.
14. Barboi, N. I., and Dilung, I. I. (1969) Electrometric study of photochemical oxidation of chlorophyll and a series of its derivatives, *Biofizika 14*, 980−985.
15. Borg, D. C., Fajer, J., Felton, R. H., and Dolphin, D. (1970) π-Cation radical of chlorophyll a, *Proc. Natl. Acad. Sci. U.S.A. 67*, 813−820.
16. Saji, T., and Bard, A. J. (1977) Electrogenerated chemiluminescence. 29. The electrochemistry and chemiluminescence of chlorophyll a in N,N-dimethylformamide solutions, *J. Am. Chem. Soc. 99*, 2235−2240.
17. Seely, G. R. (1978) The energetics of electron-transfer reactions of chlorophyll and other compounds, *Photochem. Photobiol. 27*, 639−654.
18. Davis, M. S., Forman, A., and Fajer, J. (1979) Ligated chlorophyll cation radicals: Their function in photosystem II of plant photosynthesis, *Proc. Natl. Acad. Sci. U.S.A. 76*, 4170−4174.
19. Wasielewski, M. R., Norris, J. R., Shipman, L. L., Lin, C.-P., and Svec, W. A. (1981) Monomeric chlorophyll a enol: Evidence for its possible role as the primary electron donor in photosystem I of plant photosynthesis, *Proc. Natl. Acad. Sci. U.S.A. 78*, 2957−2961.
20. Watanabe, T., and Kobayashi, M. (1991) Electrochemistry of chlorophylls, in *Chlorophylls* (Scheer, H., Ed.) pp 287−315, CRC Press, Boca Raton, FL.
21. Van Gorkom, H. J., and Schelvis, J. P. M. (1993) Kok's oxygen clock: What makes it tick? The structure of P680 and consequences of its oxidizing power, *Photosynth. Res. 38*, 297−301.
22. Diner, B. A., and Babcock, G. T. (1996) Structure, dynamics, and energy conversion efficiency in photosystem II, in *Oxygenic Photosynthesis: The Light Reactions* (Ort, D. R., and Yocum, C. F., Eds.) pp 213−247, Kluwer, Dordrecht, The Netherlands.
23. Mulkidjanian, A. Y. (1999) Photosystem II of green plants: On the possible role of retarded protonic relaxation in water oxidation, *Biochim. Bioiphys. Acta 1410*, 1−6.
24. Lubitz, W., Lendzian, F., and Bittl, R. (2002) Radicals, radical pairs and triplet states in photosynthesis, *Acc. Chem. Res. 35*, 313−320.
25. Renger, G., and Holzwarth, A. R. (2005) Primary electron transfer, in *The Water/Plastoquinone Oxido-Reductase of Photosynthesis* (Wydrzynski, T., and Satoh, K., Eds.) Kluwer, Dordrecht, The Netherlands (in press).
26. Artz, K., Williams, J. C., Allen, J. P., Lendzian, F., Rautter, J., and Lubitz, W. (1997) Relationship between the oxidation potential and electron spin density of the primary electron donor in reaction centers from *Rhodobacter sphaeroides*, *Proc. Natl. Acad. Sci. U.S.A. 94*, 13582−13587.
27. Ivancich, A., Artz, K., Williams, J. C., Allen, J. P., and Mattioli, T. A. (1998) Effects of hydrogen bonds on the redox potential and electronic structure of the bacterial primary electron donor, *Biochemistry 37*, 11812−11820.
28. Reimers, J. R., Hughes, J. M., and Hush, N. S. (2000) Modeling the bacterial photosynthetic reaction center 3: Interpretation of effects of site-directed mutagenesis on the special-pair midpoint potential, *Biochemistry 39*, 16185−16189.
29. Müh, F., Lendzian, F., Roy, M., Williams, J. C., Allen, J. P., and Lubitz, W. (2002) Pigment−protein interactions in bacterial reaction centers and their influence on oxidation potential and spin density distribution of the primary donor, *J. Phys. Chem. B 106*, 3226−3236.
30. Rigby, S. E. J., Nugent, J. H. A., and O'Malley, P. J. (1994) ENDOR and special triple-resonance studies of chlorophyll cation radicals in photosystem-2, *Biochemistry 33*, 10043−10050.
31. Matysik, J., Alia, G. P., van Gorkom, H. J., Hoff, A. J., and de Groot, H. J. M. (2000) Photochemically induced nuclear spin polarization in reaction centers of photosystem II observed by C-13-solid-state NMR reveals a strongly asymmetric electronic structure of the P-680$^{\bullet+}$ primary donor chlorophyll, *Proc. Natl. Acad. Sci. U.S.A. 97*, 9865−9870.
32. Diner, B. A., Schlodder, E., Nixon, P. J., Coleman, W. J., Rappaport, F., Lavergne, J., Vermaas, W. F. J., and Chisholm, D. A. (2001) Site-directed mutations at D1-His198 and D2-His 97 of photosystem II in *Synechocystis* PCC 6803: Sites of primary charge separation and cation and triplet stabilization, *Biochemistry 40*, 9265−9281.
33. Ferreira, K. N., Iverson, T. M., Maghlaoui, K., Barber, J., and Iwata, S. (2004) Architecture of the photosynthetic oxygen-evolving center, *Science 303*, 1831−1838.
34. Johnson, E. T., and Parson, W. W. (2002) Electrostatic interactions in an integral membrane protein, *Biochemistry 41*, 6483−6494.
35. Johnson, E. T., Nagarajan, V., Zazubovich, V., Riley, K., Small, G. J., and Parson, W. W. (2003) Effects of ionizable residues on the absorption spectrum and initial electron-transfer kinetics in the photosynthetic reaction center of *Rhodobacter sphaeroides*, *Biochemistry 42*, 13673−13683.
36. Sharp, K. A., and Honig, B. (1990) Electrostatic interactions in macromolecules: Theory and applications, *Annu. Rev. Biophys. Biophys. Chem. 19*, 301−332.
37. Steffen, M. A., Lao, K., and Boxer, S. G. (1994) Dielectric asymmetry in the photosynthetic reaction center, *Science 264*, 810−816.
38. Simonson, T., and Brooks, C. L., III (1996) Charge screening and the dielectric constant of proteins: Insights from molecular dynamics, *J. Am. Chem. Soc. 118*, 8452−8458.
39. Krishtalik, L. I., Kuznetsov, A. M., and Mertz, E. L. (1997) Electrostatics of proteins: Description in terms of two dielectric constants simultaneously, *Proteins 28*, 174−182.
40. Rabenstein, B., Ullmann, G. M., and Knapp, E.-W. (1998) Calculation of protonation patterns in proteins with structural relaxation and molecular ensembles: Application to the photosynthetic reaction center, *Eur. Biophys. J. 27*, 626−637.
41. Mertz, E. L., and Krishtalik, L. I. (2000) Low dielectric response in enzyme active site, *Proc. Natl. Acad. Sci. U.S.A. 97*, 2081−2086.
42. Ishikita, H., Loll, B., Biesiadka, J., Saenger, W., and Knapp, E.-W. (2005) Redox potentials of chlorophylls in the photosystem II reaction center, *Biochemistry 44*, 4118−4124.
43. Blomberg, M. R. A., Siegbahn, P. E. M., and Babcock, G. T. (1998) Modeling electron transfer in biochemistry: A quantum chemical study of charge separation in *Rhodobacter sphaeroides* and photosystem II, *J. Am. Chem. Soc. 120*, 8812−8824.
44. Crystal, J., and Friesner, R. A. (2000) Calculation of the ionization potentials and electron affinities of bacteriochlorophyll and bacteriopheophytin via ab initio quantum chemistry, *J. Phys. Chem. A 104*, 2362−2366.
45. O'Malley, P. J. (2000) The effect of oxidation and reduction of chlorophyll a on its geometry, vibrational and spin density properties as revealed by hybrid density functional methods, *J. Am. Chem. Soc. 122*, 7798−7801.

46. O'Malley, P. J., and Collins, S. J. (2001) The effect of axial Mg ligation on the geometry and spin density distribution of chlorophyll and bacteriochlorophyll cation free radical models: A density functional study, *J. Am. Chem. Soc. 123*, 11042−11046.
47. Sinnecker, S., Koch, W., and Lubitz, W. (2000) Bacteriochlorophyll a radical cation and anion calculation of isotropic hyperfine coupling constants by density functional methods, *Phys. Chem. Chem. Phys. 2*, 4772−4778.
48. Sinnecker, S., Koch, W., and Lubitz, W. (2002) Chlorophyll a radical ions: A density functional study, *J. Phys. Chem. B 106*, 5281−5288.
49. Sundholm, D. (2003) A density-functional-theory study of bacteriochlorophyll b, *Phys. Chem. Chem. Phys. 5*, 4265−4271.
50. Ceccarelli, M., Procacci, P., and Marchi, M. (2003) An ab initio force field for the cofactors of bacterial photosynthesis, *J. Comput. Chem. 24*, 129−142.
51. Hasegawa, J., Ishida, M., Nakatsuji, H., Lu, Z., Liu, H., and Yang, W. (2003) Energetics of the electron transfer from bacteriopheophytin to ubiquinone in the photosynthetic reaction center of *Rhodopseudomonas viridis*: Theoretical study, *J. Phys. Chem. B 107*, 838−847.
52. Sun, Y. M., Wang, H. Z., Zhao, F. L., and Sun, J. Z. (2004) The effect of axial Mg^{2+} ligation and peripheral hydrogen bonding on chlorophyll a, *Chem. Phys. Lett. 387*, 12−16.
53. Linnanto, J., and Korppi-Tommola, J. (2004) Structural and spectroscopic properties of Mg-bacteriochlorin and methyl bacteriochlorophyllides a, b, g, and h studied by semiempirical, ab initio, and density functional molecular orbital methods, *J. Phys. Chem. A 108*, 5872−5882.
54. Zhang, L. Y., and Friesner, R. A. (1995) *Ab initio* electronic-structure calculation of the redox potentials of bacteriochlorophyll and bacteriopheophytin in solution, *J. Phys. Chem. 99*, 16479−16482.
55. Sakuma, T., Kashiwagi, H., Takeda, T., and Nakamura, H. (1997) Ab initio MO study of the chlorophyll dimer in the photosynthetic reaction center. 1. A theoretical treatment of the electrostatic field created by the surrounding proteins, *Int. J. Quantum Chem. 61*, 137−151.
56. Datta, S. N., Parandekar, P. V., and Lochan, R. C. (2001) Identity of green plant reaction centers from quantum chemical determination of redox potentials of special pairs, *J. Phys. Chem. B 105*, 1442−1451.
57. Frisch, M. J., Trucks, G. W., Schlegel, H. B., Scuseria, G. E., Robb, M. A., Cheeseman, J. R., Montgomery, J. A., Jr., Vreven, T., Kudin, K. N., Burant, J. C., Millam, J. M., Iyengar, S. S., Tomasi, J., Barone, V., Mennucci, B., Cossi, M., Scalmani, G., Rega, N., Petersson, G. A., Nakatsuji, H., Hada, M., Ehara, M., Toyota, K., Fukuda, R., Hasegawa, J., Ishida, M., Nakajima, T., Honda, Y., Kitao, O., Nakai, H., Klene, M., Li, X., Knox, J. E., Hratchian, H. P., Cross, J. B., Adamo, C., Jaramillo, J., Gomperts, R., Stratmann, R. E., Yazyev, O., Austin, A. J., Cammi, R., Pomelli, C., Ochterski, J. W., Ayala, P. Y., Morokuma, K., Voth, G. A., Salvador, P., Dannenberg, J. J., Zakrzewski, V. G., Dapprich, S., Daniels, A. D., Strain, M. C., Farkas, O., Malick, D. K., Rabuck, A. D., Raghavachari, K., Foresman, J. B., Ortiz, J. V., Cui, Q., Baboul, A. G., Clifford, S., Cioslowski, J., Stefanov, B. B., Liu, G., Liashenko, A., Piskorz, P., Komaromi, I., Martin, R. L., Fox, D. J., Keith, T., Al-Laham, M. A., Peng, C. Y., Nanayakkara, A., Challacombe, M., Gill, P. M. W., Johnson, B., Chen, W., Wong, M. W., Gonzalez, C., and Pople, J. A. (2003) *Gaussian 03*, revision B.03, Gaussian, Inc., Pittsburgh, PA.
58. Chow, H.-C., Serlin, R., and Strouse, C. E. (1975) Crystal and molecular structure and absolute configuration of ethyl chlorophyllide a-dihydrate. Model for the different spectral forms of chlorophyll a, *J. Am. Chem. Soc. 97*, 7230−7237.
59. Becke, A. D. (1993) Density-functional thermochemistry. III. The role of exact exchange, *J. Chem. Phys. 98*, 5648−5652.
60. Lee, C., Yang, W., and Parr, R. G. (1988) Development of the Colle-Salvetti correlation-energy formula into a functional of the electron density, *Phys. Rev. B 37*, 785−789.
61. Cances, E., Mennucci, B., and Tomasi, J. (1997) A new integral equation formalism for the polarizable continuum model: Theoretical background and applications to isotropic and anisotropic dielectrics, *J. Chem. Phys. 107*, 3032−3041.
62. Mennucci, B., and Tomasi, J. (1997) Continuum solvation models: A new approach to the problem of solute's charge distribution and cavity boundaries, *J. Chem. Phys. 106*, 5151−5158.
63. Mennucci, B., Cances, E., and Tomasi, J. (1997) Evaluation of solvent effects in isotropic and anisotropic dielectrics and in ionic solutions with a unified integral equation method: Theoretical bases, computational implementation, and numerical applications, *J. Phys. Chem. B 101*, 10506−10517.
64. Nakato, Y., Chiyoda, T., and Tsubomura, H. (1974) Experimental determination of ionization potentials of organic amines, β-carotene and chlorophyll a, *Bull. Chem. Soc. Jpn. 47*, 3001−3005.
65. Spangler, D., Maggiora, G. M., Shipman, L. L., and Christoffersen, R. E. (1977) Stereoelectronic properties of photosynthetic and related systems. 2. Ab initio quantum mechanical ground state characterization of magnesium porphine, magnesium chlorin, and ethyl chlorophyllide a, *J. Am. Chem. Soc. 99*, 7478−7489.
66. Kashiwagi, H., Hirota, F., Nagashima, U., and Takada, T. (1986) Ab initio MO calculations on the chlorophyll-water system and estimation of the structure of the special pair, *Int. J. Quantum Chem. 30*, 311−326.
67. Torres, R. A., Lovell, T., Noodleman, L., and Case, D. A. (2003) Density functional and reduction potential calculations of Fe_4S_4 clusters, *J. Am. Chem. Soc. 125*, 1923−1936.
68. Trasatti, S. (1986) The absolute electrode potential: An explanatory note, *Pure Appl. Chem. 58*, 955−966.
69. Reiss, H., and Heller, A. (1985) The absolute potential of the standard hydrogen electrode: A new estimate, *J. Phys. Chem. 89*, 4207−4213.
70. Curtiss, L. A., Redfern, P. C., Raghavachari, K., and Pople, J. A. (1998) Assessment of Gaussian-2 and density functional theories for the computation of ionization potentials and electron affinities, *J. Chem. Phys. 109*, 42−55.
71. Staroverov, V. N., Scuseria, G. E., Tao, J. M., and Perdew, J. P. (2003) Comparative assessment of a new nonempirical density functional: Molecules and hydrogen-bonded complexes, *J. Chem. Phys. 119*, 12129−12137.
72. Born, M. (1920) Volumen und hydratationswärme der ionen, *Z. Phys. 1*, 45−48.
73. Sétif, P., and Mathis, P. (1980) The oxidation−reduction potential of P-700 in chloroplast lamellae and subchloroplast particles, *Arch. Biochem. Biophys. 204*, 477−485.
74. Chipot, C., Maigret, B., Rivail, J.-L., and Scheraga, H. A. (1992) Modeling amino acid side chains. 1. Determination of net atomic charges from ab initio self-consistent-field molecular electrostatic properties, *J. Phys. Chem. 96*, 10276−10284.
75. Stowell, M. H. B., Mcphillips, T. M., Soltis, S. M., Rees, D. C., Abresch, E., and Feher, G. (1997) Light-induced structural changes in photosynthetic reaction center: Implications for mechanism of electron−proton transfer, *Science 276*, 812−816.
76. Jordan, P., Fromme, P., Witt, H. T., Klukas, O., Saenger, W., and Krauss, N. (2001) Three-dimensional structure of cyanobacterial photosystem I at 2.5 Å resolution, *Nature 411*, 909−917.
77. Deisenhofer, J., Epp, O., Sinning, I., and Michel, H. (1995) Crystallographic refinement at 2.3 Å resolution and refined model of the photosynthetic reaction center from *Rhodopseudomonas viridis*, *J. Mol. Biol. 246*, 429−457.
78. Allen, J. P., Artz, K., Lin, X., Williams, J. C., Ivancich, A., Albouy, D., Mattioli, T. A., Fetsch, A., Kuhn, M., and Lubitz, W. (1996) Effects of hydrogen bonding to a bacteriochlorophyll-bacteriopheophytin dimer in reaction centers from *Rhodobacter sphaeroides*, *Biochemistry 35*, 6612−6619.
79. Laporte, L., McDowell, L. M., Kirmaier, C., Schenck, C. C., and Holten, D. (1993) Insights into the factors controlling the rates of the deactivation processes that compete with charge separation in photosynthetic reaction centers, *Chem. Phys. 176*, 615−629.
80. Laporte, L. L., Palaniappan, V., Davis, D. G., Kirmaier, C., Schenck, C. C., Holten, D., and Bocian, D. F. (1996) Influence of electronic asymmetry on the spectroscopic and photodynamic properties of the primary electron donor in the photosynthetic reaction center, *J. Phys. Chem. 100*, 17696−17707.
81. Pantelidou, M., Chitnis, P. R., and Breton, J. (2004) FTIR spectroscopy of *Synechocystis* 6803 mutants affected on the hydrogen bonds to the carbonyl groups of the PsaA chlorophyll of P700 supports an extensive delocalization of the charge in P700, *Biochemistry 43*, 8380−8390.
82. Webber, A. N., and Lubitz, W. (2001) P700: The primary electron donor of photosystem I, *Biochim. Bioiphys. Acta 1507*, 61−79.
83. Reimers, J. R., Hutter, M. C., Hughes, J. M., and Hush, N. S. (2000) Nature of the special-pair radical cation in bacterial photosynthesis, *Int. J. Quantum Chem. 80*, 1224−1243.

84. Plato, M., Krauss, N., Fromme, P., and Lubitz, W. (2003) Molecular orbital study of the primary electron donor P700 of photosystem I based on a recent X-ray single-crystal structure analysis, *Chem. Phys. 294*, 483−499.
85. Biesiadka, J., Loll, B., Kern, J., Irrgang, K. D., and Zouni, A. (2004) Crystal structure of cyanobacterial photosystem II at 3.2 Å resolution: A closer look at the Mn-cluster, *Phys. Chem. Chem. Phys. 6*, 4733−4736.
86. Noguchi, T., Tomo, T., and Inoue, Y. (1998) Fourier transform infrared study of the cation radical of P680 in the photosystem II reaction center: Evidence for charge delocalization on the chlorophyll dimer, *Biochemistry 37*, 13614−13625.
87. Breton, J. (2001) Fourier transform infrared spectroscopy of primary electron donors in type I photosynthetic reaction centers, *Biochim. Biophys. Acta 1507*, 180−193.
88. Fajer, J. (2004) Chlorophyll chemistry before and after crystals of photosynthetic reaction centers, *Photosynth. Res. 80*, 165−172.

BI050273C